

Universal Joints and Driveshafts

H. Chr. Seherr-Thoss · F. Schmelz · E. Aucktor

H. Chr. Seherr-Thoss · F. Schmelz · E. Aucktor

Universal Joints and Driveshafts

Analysis, Design, Applications

Second, enlarged edition with 267 Figures and 72 Tables

Translated by J. A. Tipper and S. J. Hill



Springer

Authors:

HANS CHRISTOPH SEHERR-THOSS, Dipl.-Ing.
Holder of the Graf Seherr Archives, Unterhaching

FRIEDRICH SCHMELZ, Dipl.-Ing.
Test- and Computing Engineer, Ingolstadt

ERICH AUCKTOR, Dipl.-Ing.
Development- and Design-Engineer, Offenbach a.M.

Translators:

MRS. JENNIFER A. TIPPER
B.A. HONS., LICHFIELD

DR. STUART J. HILL, B. A. (Eng.)
HONS. PH. D., British Railways Board, London

ISBN-10 3-540-30169-0 Springer-Verlag Berlin Heidelberg New York
ISBN-13 978-3-540-30169-1 Springer-Verlag Berlin Heidelberg New York

Library of Congress Cataloging-in-Publication Data

[Gelenke and Gelenkwellen. English]

Universal joints and driveshafts: analysis, design, applications/F. Schmelz

H. Chr. Seherr-Thoss, E. Aucktor; translated by S. J. Hill and

J. A. Tipper. p. cm.

Translation of: Gelenke und Gelenkwellen. Includes indexes.

ISBN 3-540-41759-1

1. Universal joints. 2. Automobiles – Powertrains.

I. Seherr-Thoss, H.-Chr. (Hans-Christoph), Count, II. Schmelz, F.

(Friedrich), III. Aucktor, E. (Erich), 1913–98.

TJ1059.S3613 1992 621.8'25—dc20 90-28614

This work is subject to copyright. All rights are reserved, whether the whole or part of the material is concerned, specifically the rights of translation, reprinting, reuse of illustrations, recitation, broadcasting, reproduction on microfilm or in any other way, and storage in data banks. Duplication of this publication or parts thereof is permitted only under the provisions of the German Copyright Law of September 9, 1965, in its current version, and permission for use must always be obtained from Springer-Verlag. Violations are liable for prosecution under the German Copyright Law.

Springer is a part of Springer Science+Business Media

springer.com

© Springer-Verlag Berlin Heidelberg 2006

Printed in Germany

The use of registered names, trademarks, etc. in this publication does not imply, even in the absence of a specific statement, that such names are exempt from the relevant protective laws and regulations and therefore free for general use.

Typesetting: Fotosatz-Service Köhler GmbH, Würzburg

Projectmanagement: Reinhold Schöberl, Würzburg

Cover design: medionet AG, Berlin

Printed on acid-free paper – 62/3020 – 543210

Preface to the second English edition

An important date in the history of automotive engineering was celebrated at the start of the 1980s: 50 years of front-wheel drives in production vehicles. This bicentennial event aroused interest in the development, theory and future of driveshafts and joints. The authors originally presented all the available knowledge on constant-velocity and universal-joint driveshafts in German as long ago as 1988, followed by English in 1992 and Chinese in 1997.

More than ten years have passed since then, in which time technology has also made major progress in the field of driveshafts. Driveshaft design and manufacturing process has kept pace with the constantly growing demands of the various users. More powerful engines with higher torques, new fields of application with increased stresses, e.g. off-road and heavy goods vehicles or rolling mills, improved materials, new production processes and advanced experimental and test methods have imposed completely new requirements on the driveshaft as a mechanical component.

GKN Driveline has made a major contribution to the further development of the driveshaft and will maintain this effort in the future. At our Research & Product Development Centres, GKN engineers have defined basic knowledge and conceived product improvements for the benefit of the automotive, agricultural, and machinery industry of mechanically engineered products for the world. In close cooperation with its customers GKN has created low-noise, vibration and maintenance-free driveshafts.

The cumulative knowledge acquired has been compiled in this second edition book that has been updated to reflect the latest state of the art. It is intended to serve both as a textbook and a work of reference for all driveline engineers, designers and students who are in some way involved with constant-velocity and universal-joint driveshafts.

Redditch, England
July 2005

ARTHUR CONNELLY
Chief Executive Officer
GKN Automotive Driveline Driveshafts

Preface to the second German edition

1989 saw the start of a new era of the driveline components and driveshafts, driven by changing customer demands. More vehicles had front wheel drive and transverse engines, which led to considerable changes in design and manufacture, and traditional methods of production were revisited. The results of this research and development went into production in 1994–96:

- for Hooke’s jointed driveshafts, weight savings were achieved through new forgings, noise reduction through better balancing and greater durability through improved lubrication.
- for constant velocity joints, one can talk about a “New Generation”, employing something more like roller bearing technology, but where the diverging factors are dealt with. The revised Chapters 4 and 5 re-examine the movement patterns and stresses in these joints.

The increased demands for strength and precision led to even intricate shapes being forged or pressed. These processes produce finished parts with tolerances of 0.025 mm. 40 million parts were forged in 1998. These processes were also reviewed.

Finally, advances were made in combined Hooke’s and constant velocity jointed driveshafts.

A leading part in these developments was played by the GKN Group in Birmingham and Lohmar, which has supported the creation of this book since 1982. As a leading manufacturer they supply 600,000 Hooke’s jointed driveshafts and 500,000 constant velocity driveshafts a year. I would like to thank REINHOLD SCHOEBERL for his project-management and typography to carry out the excellent execution of this book.

I would also like to thank my wife, THERESE, for her elaboration of the indices. Moreover my thanks to these contributors:

GERD FAULBECKER (GWB Essen)
JOACHIM FISCHER (ZF Lenksysteme Gmünd)
WERNER JACOB (Ing. Büro Frankfurt/M)
CHRISTOPH MÜLLER (Ing. Büro Ingolstadt)
PROF. DR. ING. ERNST-GÜNTER PALAND (TU Hannover, IMKT)
JÖRG PAPENDORF (Spicer GWB Essen)
STEFAN SCHIRMER (Freudenberg)
RALF SEDLMEIER (GWB Essen)
ARMIN WEINHOLD (SMS Eumuco Düsseldorf/Leverkusen)

GKN Driveline (Lohmar/GERMANY)

WOLFGANG HILDEBRANDT

WERNER KRUDE

STEPHAN MAUCHER

MICHAEL MIRAU (Offenbach)

CLEMENS NIENHAUS (Walterscheid)

PETER POHL (Walterscheid Trier)

RAINER SCHAEFERDIEK

KARL-ERNST STROBEL (Offenbach)

On 19th July 1989 our triumvirate lost Erich Aucktor. He made a valuable contribution to the development of driveline technology from 1937–1958, as an engine engineer, and from 1958–78 as a designer and inventor of constant velocity joints at Löhrl & Bromkamp, Offenbach, where he worked in development, design and testing. It is thanks to him that this book has become a reference work for these engineering components.

COUNT HANS CHRISTOPH SEHERR-THOSS

Contents

Index of Tables	XIII
Notation	XVII
Chronological Table	XXI
Chapter 1 Universal Jointed Driveshafts for Transmitting	
Rotational Movements	1
1.1 Early Reports on the First Joints	1
1.1.1 Hooke's Universal Joints	1
1.2 Theory of the Transmission of Rotational Movements by Hooke's Joints	5
1.2.1 The Non-univormity of Hooke's Joints According to Poncelet . . .	5
1.2.2 The Double Hooke's Joint to Avoid Non-univormity	8
1.2.3 D'Ocagne's Extension of the Conditions for Constant Velocity . .	10
1.2.4 Simplification of the Double Hooke's Joint	10
1.2.4.1 Fenaille's Tracta Joint	12
1.2.4.2 Various Further Simplifications	14
1.2.4.3 Bouchard's One-and-a-half Times Universal Joint	14
1.3 The Ball Joints	17
1.3.1 Weiss and Rzeppa Ball Joints	19
1.3.2 Developments Towards the Plunging Joint	27
1.4 Development of the Pode-Joints	32
1.5 First Applications of the Science of Strength of Materials to Driveshafts	40
1.5.1 Designing Crosses Against Bending	40
1.5.2 Designing Crosses Against Surface Stress	42
1.5.3 Designing Driveshafts for Durability	47
1.6 Literature to Chapter 1	49
Chapter 2 Theory of Constant Velocity Joints (CVJ)	53
2.1 The Origin of Constant Velocity Joints	54
2.2 First Indirect Method of Proving Constant Velocity According to Metzner	58
2.2.1 Effective Geometry with Straight Tracks	61
2.2.2 Effective Geometry with Circular Tracks	64

2.3	Second, Direct Method of Proving Constant Velocity by Orain . . .	66
2.3.1	Polypode Joints	71
2.3.2	The Free Tripode Joint	75
2.4	Literature to Chapter 2	78
Chapter 3 Hertzian Theory and the Limits of Its Application		81
3.1	Systems of Coordinates	82
3.2	Equations of Body Surfaces	83
3.3	Calculating the Coefficient $\cos \tau$	85
3.4	Calculating the Deformation δ at the Contact Face	88
3.5	Solution of the Elliptical Single Integrals J_1 to J_4	94
3.6	Calculating the Elliptical Integrals K and E	97
3.7	Semiaxes of the Elliptical Contact Face for Point Contact	98
3.8	The Elliptical Coefficients μ and ν	101
3.9	Width of the Rectangular Contact Surface for Line Contact	101
3.10	Deformation and Surface Stress at the Contact Face	104
3.10.1	Point Contact	104
3.10.2	Line Contact	105
3.11	The validity of the Hertzian Theory on ball joints	106
3.12	Literature to Chapter 3	107
Chapter 4 Designing Joints and Driveshafts		109
4.1	Design Principles	109
4.1.1	Comparison of Theory and Practice by Franz Karas 1941	110
4.1.2	Static Stress	111
4.1.3	Dynamic Stress and Durability	112
4.1.4	Universal Torque Equation for Joints	114
4.2	Hooke's Joints and Hooke's Jointed Driveshafts	116
4.2.1	The Static Torque Capacity M_o	117
4.2.2	Dynamic Torque Capacity M_d	118
4.2.3	Mean Equivalent Compressive Force P_m	119
4.2.4	Approximate Calculation of the Equivalent Compressive Force P_m	124
4.2.5	Dynamic Transmission Parameter $2 CR$	126
4.2.5.1	Example of Specifying Hooke's Jointed Driveshafts in Stationary Applications	128
4.2.6	Motor Vehicle Driveshafts	130
4.2.7	GWB's Design Methodology for Hooke's joints for vehicles	133
4.2.7.1	Example of Specifying Hooke's Jointed Driveshafts for Commercial Vehicles	136
4.2.8	Maximum Values for Speed and Articulation Angle	138
4.2.9	Critical Speed and Shaft Bending Vibration	140
4.2.10	Double Hooke's Joints	144
4.3	Forces on the Support Bearings of Hooke's Jointed Driveshafts	148
4.3.1	Interaction of Forces in Hooke's Joints	148
4.3.2	Forces on the Support Bearings of a Driveshaft in the W-Configuration	150

4.3.3	Forces on the Support Bearings of a Driveshaft in the Z-Configuration	152
4.4	Ball Joints	153
4.4.1	Static and Dynamic Torque Capacity	154
4.4.1.1	Radial bearing connections forces	158
4.4.2	The ball-joint from the perspective of rolling and sliding bearings	158
4.4.3	A common, precise joint centre	159
4.4.3.1	Constant Velocity Ball Joints based on Rzeppa principle	160
4.4.4	Internal centering of the ball-joint	162
4.4.4.1	The axial play s_a	163
4.4.4.2	Three examples for calculating the axial play s_a	164
4.4.4.3	The forced offset of the centre	166
4.4.4.4	Designing of the spherical contact areas	169
4.4.5	The geometry of the tracks	170
4.4.5.1	Longitudinal sections of the tracks	170
4.4.5.2	Shape of the Tracks	174
4.4.5.3	Steering the Balls	177
4.4.5.4	The Motion of the Ball	178
4.4.5.5	The cage in the ball joint	179
4.4.5.6	Supporting surface of the cage in ball joints	183
4.4.5.7	The balls	184
4.4.5.8	Checking for perturbations of motion in ball joints	185
4.4.6	Structural shapes of ball joints	187
4.4.6.1	Configuration and torque capacity of Rzeppa-type fixed joints . .	187
4.4.6.2	AC Fixed Joints	188
4.4.6.3	UF Fixed joints (undercut free)	193
4.4.6.4	Jacob/Paland's CUF (completely undercut free) Joint for rear wheel drive $> 25^\circ$	195
4.4.6.5	Calculation example for a CUF joint	197
4.4.7	Plunging Joints	200
4.4.7.1	DO Joints	200
4.4.7.2	VL Joints	202
4.4.8	Service Life of Joints Using the Palmgren/Miner Rule	207
4.5	Pode Joints	209
4.5.1	Bipode Plunging Joints	213
4.5.2	Tripode Joints	214
4.5.2.1	Static Torque Capacity of the Non-articulated Tripode Joint	215
4.5.2.2	Materials and Manufacture	215
4.5.2.3	GI Plunging Tripode Joints	220
4.5.2.4	Torque Capacity of the Articulated Tripode Joint	222
4.5.3	The GI-C Joint	228
4.5.4	The low friction and low vibration plunging tripod joint AAR . .	229
4.6	Materials, Heat Treatment and Manufacture	231
4.6.1	Stresses	231
4.6.2	Material and hardening	236
4.6.3	Effect of heat treatment on the transmittable static and dynamic torque	238

4.6.4	Forging in manufacturing	239
4.6.5	Manufacturing of joint parts	240
4.7	Basic Procedure for the Applications Engineering of Driveshafts	243
4.8	Literature to Chapter 4	245
Chapter 5 Joint and Driveshaft Configurations		249
5.1	Hooke's Jointed Driveshafts	250
5.1.1	End Connections	251
5.1.2	Cross Trunnions	253
5.1.3	Plunging Elements	258
5.1.4	Friction in the driveline – longitudinal plunges	258
5.1.5	The propshaft	262
5.1.6	Driveshaft tubes made out of composite Fibre materials	263
5.1.7	Designs of Driveshaft	267
5.1.7.1	Driveshafts for Machinery and Motor Vehicles	267
5.1.8	Driveshafts for Steer Drive Axles	268
5.2	The Cardan Compact 2000 series of 1989	269
5.2.1	Multi-part shafts and intermediate bearings	273
5.2.2	American Style Driveshafts	275
5.2.3	Driveshafts for Industrial use	277
5.2.4	Automotive Steering Assemblies	285
5.2.5	Driveshafts to DIN 808	292
5.2.6	Grooved Spherical Ball Jointed Driveshafts	294
5.3	Driveshafts for Agricultural Machinery	296
5.3.1	Types of Driveshaft Design	297
5.3.2	Requirements to meet by Power Take Off Shafts	298
5.3.3	Application of the Driveshafts	300
5.4	Calculation Example for an Agricultural Driveshaft	307
5.5	Ball Jointed Driveshafts	308
5.5.1	Boots for joint protection	310
5.5.2	Ways of connecting constant velocity joints	311
5.5.3	Constant velocity drive shafts in front and rear wheel drive passenger cars	312
5.5.4	Calculation Example of a Driveshaft with Ball Joints	316
5.5.5	Tripode Jointed Driveshaft Designs	321
5.5.6	Calculation for the Tripode Jointed Driveshaft of a Passenger Car	322
5.6	Driveshafts in railway carriages	325
5.6.1	Constant velocity joints	325
5.7	Ball jointed driveshafts in industrial use and special vehicles	327
5.8	Hooke's jointes high speed driveshafts	329
5.9	Design and Configuration Guidelines to Optimise the Drivetrain	332
5.9.1	Exemple of a Calculation for the Driveshafts of a Four Wheel Drive Passenger Car (Section 5.5.4)	333
5.10	Literature to Chapter 5	343

Index of Tables

Independent Tables

Table 1.1	Bipode joints 1902–52	33
Table 1.2	Tripode joints 1935–60	36
Table 1.3	Quattropode-joints 1913–94	39
Table 1.4	Raised demands to the ball joints by the customers	39
Table 3.1	Complete elliptical integrals by A.M. Legendre 1786	96
Table 3.2	Elliptical coefficients according to Hertz	102
Table 3.3	Hertzian Elliptical coefficients	103
Table 4.1	Geometry coefficient f_1 according to INA	120
Table 4.2	Shock or operating factor f_{ST}	127
Table 4.3	Values for the exponents n_1 and n_2 after GWB	138
Table 4.4	Maximum Speeds and maximum permissible values of $n\beta$ arising from the moment of inertia of the connecting parts	139
Table 4.5	Radial bearing connection forces of Constant Velocity Joints (CVJ) with shafts in one plane, from Werner KRUDE . . .	157
Table 4.6	Most favourable track patterns for the two groups of joints . . .	174
Table 4.7	Ball joint family tree	176
Table 4.8	Steering the balls in ball joints	177
Table 4.9	Effect of the ball size on load capacity and service life	185
Table 4.10	Rated torque M_N of AC joints	191
Table 4.11	Dynamic torque capacity M_d of AC joints	191
Table 4.12	Data for UF-constant velocity joints made by GKN Löbro	194
Table 4.13	VL plunging joint applications	206
Table 4.14	Percentage of time in each gear on various types of roads . . .	208
Table 4.15	Percentage of time a_x for passenger cars	208
Table 4.16	Surface stresses in poded joints with roller bearings	212
Table 4.17	Surface stresses in poded joints with plain bearings	212
Table 4.18	Materials and heat treatments of inner and outer races for UF-constant velocity joints	234
Table 4.19	Values for the tri-axial stress state and the required hardness of a ball in the track of the UF-joint	235
Table 4.20	Hardness conditions for the joint parts	238
Table 4.21	Static and dynamic torque capacities for UF constant velocity joints with outer race surface hardness depth (Rht) of 1.1 and 2.4 mm	239

Table 4.22	Applications Engineering procedure for a driveshaft with uniform loading	244
Table 5.1	Maximum articulation angle β_{\max} of joints	250
Table 5.2	Examples of longitudinal plunge via balls in drive shafts	260
Table 5.3	Data for composite propshafts for motor vehicles	263
Table 5.4	Comparison of steel and glass fibre reinforced plastic propshafts for a high capacity passenger car	267
Table 5.5	Torque capacity of Hooke's jointed driveshafts	268
Table 5.6	Steering joint data	287
Table 5.7	Comparison of driveshafts	309
Table 5.8	Examples of standard longshaft systems for passenger cars around 1998	312
Table 5.9	Durability values for the selected tripod joint on rear drive	324
Table 5.10	Comparison of a standard and a high speed driveshaft (Fig. 5.83, 5.85)	331
Table 5.11	Durability values for front wheel drive with UF 1300	335
Table 5.12	Calculation of the starting and adhesion torques in the calculation example (Section 5.9.1)	336
Table 5.13	Values for the life of the propshaft for rear wheel drive	339

Tables of principal dimensions, torque capacities and miscellaneous data inside the Figures

Figure 1.13	Pierre Fenaille's Tracta joint 1927	13
Figure 1.16	One-and-a-half times universal joint 1949	16
Figure 1.21	Fixed joint of the Weiss type	21
Figure 4.5	Bearing capacity coefficient f_2 of rolling bearings	121
Figure 4.10	Principal and cross dimensions of a Hooke's jointed driveshaft for light loading	128
Figure 4.45	Tracks with elliptical cross section	175
Figure 4.58	AC fixed joints of the Rzeppa type according to Wm. Cull	189
Figure 4.59	AC fixed joint (improved) 1999	190
Figure 4.61	UF-constant velocity fixed joint (wheel side)	195
Figure 4.64	Six-ball DO plunging joints (Rzeppa type)	201
Figure 4.65	Five-ball DOS plunging joint from Girguis 1971	202
Figure 4.66	VL plunging joints of the Rzeppa type with inclined tracks and 6 balls	203
Figure 4.77	Glaenger Spicer GE tripod joint with $\beta_{\max} = 43^\circ$ to 45°	217
Figure 4.79	Glaenger Spicer GI tripod joint	220
Figure 4.87	Plunging tripod joint (AAR)	229
Figure 5.3	Driveshaft flange connections	252
Figure 5.8	Levels of balancing quality Q for driveshafts	257
Figure 5.24	Non-centred double Hooke's jointed driveshaft with stubshaft for steer drive axles	271
Figure 5.27	Specifications and physical data of Hooke's joints for commercial vehicles with length compensation	274

Figure 5.29	Hooke's jointed driveshaft from Mechanics/USA	277
Figure 5.30	Centred double-joint for high and variable articulation angles .	278
Figure 5.31	Driving dog and connection kit of a wing bearing driveshaft . .	279
Figure 5.32	Specifications, physical data and dimensions of the cross trunnion of a Hooke's jointed driveshaft for stationary (industrial) use	280
Figure 5.33	Universal joints crosses for medium and heavy industrial shafts	281
Figure 5.34	Specifications, physical data and dimensions of the cross trunnion of Hooke's jointed driveshafts for industrial use, heavy type with length compensation and dismantable bearing cocer	282
Figure 5.35	Specifications of Hooke's heavy driveshafts with length compensation and flange connections for rolling-mills and other big machinery	282
Figure 5.40	Full complement roller bearing. Thin wall sheet metal bush . .	287
Figure 5.42	Steering joints with sliding serration ca. 1970	289
Figure 5.46	Single and double joint with plain and needle bearings	292
Figure 5.51	Connection measurement for three tractor sizes from ISO standards	296
Figure 5.55	Joint sizes for agricultural applications	299
Figure 5.56	Sizes for sliding profiles of driveshafts on agricultural machinery	301
Figure 5.58	Hooke's joints in agricultural use with protection covers	302
Figure 5.61	Double joints with misaligned trunnions	305
Figure 5.70	Drive shafts with CV joints for Commercial and Special vehicles	315

Notation

Symbol	Unit	Meaning
1. Coordinate Systems		
$0, x, y, z$	mm	orthogonal, right-handed body system
$0, x', y', z'$	mm	spatial system, arising from the transformation with the rotation matrix $D_\varphi = \begin{pmatrix} \sin \varphi & -\cos \varphi & 0 \\ \cos \varphi & \sin \varphi & 0 \\ 0 & 0 & 1 \end{pmatrix}$
$0, x'', y'', z''$	mm	spatial system, arising from the transformation with the translation matrix $D_\beta = \begin{pmatrix} 1 & 0 & 0 \\ 0 & \cos \beta & -\sin \beta \\ 0 & \sin \beta & \cos \beta \end{pmatrix}$
$0, r, \varphi$ $r = a + tu$	mm, degrees	system of polar coordinates in Boussinesq half space vectorial representation of a straight track
$a = \begin{pmatrix} k \\ l \\ m \end{pmatrix}$		location vector and its components
$u = \begin{pmatrix} n \\ p \\ q \end{pmatrix}$		direction vector and its components
Indices 1		body 1, driving unit
Indices 2		body 2, driven unit or intermediate body
Indices 3		body 3, driven unit for three bodies
$i = 1, 2, 3, \dots n$		sequential numbering

Symbol	Unit	Meaning
2. Angles		
α	degrees	pressure angle
β	degrees	articulation angle
γ	degrees	skew angle of the track
δ	degrees	divergence of opening angle ($\delta = 2\varepsilon$), offset angle
ε	degrees	tilt or inclination angle of the track (Stuber pledge angle)
ϑ	degrees	complementary angle to α ($\alpha = 90^\circ - \vartheta$)
τ	degrees	Hertzian auxiliary angle
$\cos \tau$	–	Hertzian coefficient
φ	degrees	angle of rotation through the joint body
χ	degrees	angle of intersection of the tracks
ψ	degrees	angle of the straight generators r
3. Rolling body data		
A	mm^2	contact area
$2a$	mm	major axis of contact ellipse
$2b$	mm	minor axis of contact ellipse
$2c$	mm	separation of cross axes of double Hooke's joints
c	mm	offset (displacement of generating centres)
d	mm	roller diameter
D	mm	trunnion diameter
D_m	mm	diameter of the pitch circle of the rolling bodies
k	N/mm^2	specific loading
l	mm	roller length (from catalogue)
l_w	mm	effective length of roller
r	mm	radius of curvature of rolling surfaces
R	m	effective joint radius
s_w	mm	joint plunge
ψ		reciprocal of the conformity in the track cross section
κ_Q		conformity in the track cross section
κ_L		conformity in the longitudinal section of the track
$\varrho = 1/r$	1/mm	curvature of the rolling surfaces
c_p	N/mm^2	coefficient of conformity
p_o	N/mm^2	Hertzian pressure
δ_o	mm	total elastic deformation at a contact point
δ_b	mm	plastic deformation
μ, ν		Hertzian elliptical coefficients
E	N/mm^2	Young's modulus ($2.08 \cdot 10^{11}$ for steel)
m		Poisson's ratio = 3/10
$\vartheta = \frac{4}{E} (1 - m^2)$	mm^2/N	abbreviation used by Hertz
z	–	number of balls

Symbol	Unit	Meaning
4. Forces		
P	N	equivalent dynamic compressive force
Q	N	Hertzian compressive force
F	N	radial component of equivalent compressive force P
A	N	axial component of equivalent compressive force P
Q_{total}	N	total radial force on a roller bearing used by Hertz/Stribeck
5. Moments		
M	Nm	moments in general
M_0	Nm	static moment
M_d	Nm	dynamic moment
M_N	Nm	nominal moment (from catalogue)
M_b	Nm	bending moment
M_B	Nm	design moment
6. Mathematical constants and coefficients		
ε		ratio of the front and rear axle loads A_F/A_R
ε_F		fraction of torque to the front axle
ε_R		fraction of torque to the rear axle
f_β		articulation coefficient
k_ω		equivalence factor for cyclic compressive forces
s		Stribeck's distribution factor = 5
s_0		static safety factor for oscillating bearings of Hooke's joints = 0.8 to 1.0
u		number of driveshafts
μ		friction coefficient of road
7. Other designations		
P_{eff}	kW	output power
V	kph	driving speed
ω	s^{-1}	angular velocity
m		effective number of transmitting elements
n	rpm	rotational speed (revolutions per minute)
π		plane of symmetry

Designations which have not been mentioned are explained in the text or shown in the figures.

Chronological Table

- 1352–54 Universal jointed driveshaft in the clock mechanism of Strasbourg Cathedral.
- 1550 *Gerónimo Cardano's* gimbal suspension.
- 1663 *Robert Hooke's* universal joint. 1683 double Hooke's joint.
- 1824 Analysis of the motion of Hooke's joints with the aid of spherical trigonometry and differential calculus, and the calculation of the forces on the cross by *Jean Victor Poncelet*.
- 1841 Kinematic treatment of the Hooke's joint by *Robert Willis*.
- 1894 Calculation of surface stresses for crosses by *Carl Bach*.
- 1901/02 Patents for automotive joints by *Arthur Hardt* and *Robert Schwenke*.
- 1904 Series production of Hooke's joints and driveshafts by *Clarence Winfred Spicer*.
- 1908 First ball joint by *William A. Whitney*. Plunging + articulation separated.
- 1918 Special conditions for the uniform transmission of motion by *Maurice d'Ocagne*. 1930 geometrical evidence for the constant velocity characteristics of the Tracta joint.
- 1923 Fixed ball joint steered by generating centres widely separated from the joint mid-point, by *Carl William Weiss*. Licence granted to the Bendix Corp.
- 1926 *Pierre Fenaille's* "homokinetic" joint.
- 1927 Six-ball fixed joint with 45° articulation angle by *Alfred H. Rzeppa*. 1934 with offset steering of the balls. First joint with concentric meridian tracks.
- 1928 First Hooke's joint with needle bearings for the crosses by *Clarence Winfred Spicer*. Bipode joint by *Richard Bussien*.
- 1933 Ball joint with track-offset by *Bernard K. Stuber*.
- 1935 Tripode joint by *J. W. Kittredge*, 1937 by *Edmund B. Anderson*.
- 1938 Plunging ball joint according to the offset principle by *Robert Suczek*.
- 1946 Birfield-fixed joint with elliptical tracks, 1955 plunging joint, both by *William Cull*.
- 1951 Driveshaft with separated Hooke's joint and middle sections by Borg-Warner.
- 1953 Wide angle fixed joint ($\beta = 45^\circ$) by *Kurt Schroeter*, 1971 by *H. Geisthoff*, *Heinrich Welschhof* and *H. Grosse-Entrop*.
- 1959 AC fixed joint by *William Cull* for British Motor Corp., produced by Hardy-Spicer.
- 1960 Löbro-fixed joint with semicircular tracks by *Erich Aucktor/Walter Willimek*. Tripode plunging joint, 1963 fixed joint, both by *Michel Orain*.

-
- 1961 Four-ball plunging joint with a pair of crossed tracks by *Henri Faure*.
DANA-plunging joint by *Phil. J. Mazziotti, E. H. Sharp, Zech*.
- 1962 VL-plunging joint with crossed tracks, six balls and spheric cage by *Erich Aucktor*.
- 1965 DO-plunging joint by *Gaston Devos*, completed with parallel tracks and cage offset by Birfield. 1966 series for Renault R 4.
- 1970 GI-tripode plunging joint by *Glaenger-Spicer*. UF-fixed joint by *Heinr. Welschhof/Erich Aucktor*. Series production 1972.
- 1985 Cage-guided balls for plunging in the Triplan joint by *Michel Orain*.
- 1989 AAR-joint by *Löbro* in series production.

1 Universal Jointed Driveshafts for Transmitting Rotational Movements

The earliest information about joints came from Philon of Byzantium around 230 BC in his description of censers and inkpots with articulated suspension. In 1245 AD the French church architect, Villard de Honnecourt, sketched a small, spherical oven which was suspended on circular rings. Around 1500, Leonardo da Vinci drew a compass and a pail which were mounted in rings [1.1].

1.1 Early Reports on the First Joints

Swiveling gimbals were generally known in Europe through the report of the mathematician, doctor and philosopher, Geronimo Cardano. He also worked in the field of engineering and in 1550 he mentioned in his book “De subtilitate libri XXI” a sedan chair of Emperor Charles V “which was mounted in a gimbal” [1.2]. In 1557 he described a ring joint in “De armillarum instrumento”. Pivots staggered by 90° connected the three rings to one another giving rise to three degrees of freedom (Fig. 1.1). This suspension and the joint formed from it were named the “cardan suspension” or the “cardan joint” after the author.

The need to transmit a rotary movement via an angled shaft arose as early as 1300 in the construction of clocktowers. Here, because of the architecture of the tower, the clockwork and the clockface did not always lie on the same axis so that the transmission of the rotation to the hands had to be displaced upwards, downwards or sideways. An example described in 1664 by the Jesuit, Caspar Schott, was the clock in Strasbourg Cathedral of 1354 [1.3]. He wrote that the inclined drive could best be executed through a cross with four pivots which connected two shafts with forks (fusicinula) fitted to their ends (Fig. 1.2). The universal joint was therefore known long before Schott. He took his description from the unpublished manuscript “Chronometria Mechanica Nova” by a certain Amicus who was no longer alive. If one analyses Amicus’s joint, the close relationship between the gimbal and the universal joint can be seen clearly (Figs. 1.3a and b). The mathematics of the transmission of movement were however not clear to Schott, because he believed that one fork must rotate as quickly as the other.

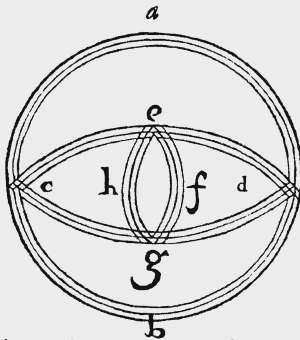
1.1.1 Hooke’s Universal Joints

In 1663 the English physicist, Robert Hooke, built a piece of apparatus which incorporated an articulated transmission not quite in the form of Amicus’s joint. In 1674 he described in his “Animadversions” [1.4] the helioscope of the Danzig astronomer,

CAPVT VII.

De Armillarum instrumento.

CONSTAT ex circulis tribus instrumen-
tum armillis simile, quorum superio-
res sunt duplicati, & polis secundus pri-
mo fixis infigitur. Vt fit A B circulus pri-
mus, cui infixi sunt ad rectos polorum CD



poli interioris, & uterque duplicatus, vel
vt media pars circumagi possit sub eisdem
polis, quia inferior; vel quia ex dimidio
stabilis præter polos, ex dimidio mobi-
lis. Tertius autem in medio secundi, ita
vt

vt circumagi possint poli eius ex E in C,
& C in G, & G in D. Et rursus polis qua-
si nullis ex E in F, & F in G, & G in H.
Et vt lateat protus coniunctio, adeo vt
annexus alter alteri videatur. Tale instru-
mentum vidi apud virum Maximiliani
Cæsaris, Mathematicum Medicum &
Philosophum insignem, Ioannem Sage-
rum Gisenhaigen Vratisleuiensem, quan-
quam neque ipse docuerit, quomodo in-
ferus esset; neque ego interrogauerim.
Ergo fieri potest, vt circulus inferior DE
CG circumuertatur, superiore immobili:
atque ita poli ferentur per E C G D: sed
tunc necessaria erit cavitates infra circulum
secundum, per quam feratur. Sed si circulus
E C G D integer fit, fieri non potest
vt ferantur poli nisi cum circulo, cui in-
fixi sint: hic autem est pars circuli prædi-
cti media, aut etiam inferior. Et tunc
ergo tres modi. Inferior autem circulus,
cum in seipso reuoluitur, poterit manen-
tibus quidem polis circumduci à lateri-
bus, fixo manente medio: nam si medius
transferatur cui polus infixus est, exibit
polus circumductus circulum E C G D
secundum latitudinem: aut transferetur
polus per cavitatem. At tunc non erit cir-
culus F G H E solidus. Cum ergo volue-
rimus circulos ambos esse solidos, relin-
quentur duo modi tantum, vt pars media
circuli secundi, cui infixi sint circuli, cir-
cumuoluantur; & extremæ inferioris par-
tes, seu latera: aut vt pars inferior secun-
di circuli intrusa superiori, & in qua sint
poli fixi edem modo sub superiore circum-
ducatur, atque eo modo totus circulus
E F G H circumagatur per E D G C. Ipse
verò circulus E D G C in seipso vt prius
manente fixa parte media, in qua sunt
poli infixi, circumducatur lateribus suis.
Commune autem est ambobus, vt poli sint
infixi vtrisque circulis secundo & tertio,
& quod latera inferioris manente medio
circumagantur. In secundo tantum differ-
runt; cum vel media pars manentibus la-
teribus, vel inferior superiore fixa circum-
duci possit.

Fig. 1.1. Ring joint of Hieronymus Cardanus 1557. In his “Mediolanensis philosophi ac medici”, p. 163, he wrote the following about it: “I saw such a device at the house of Emperor Maximilian’s adviser, Joannem Sagerum (Johann Sager) from Gisenhaigen (Gießenhagen, Geißenhain), an important mathematician, doctor and philosopher in the Pressburg diocese. He did not explain how he had arrived at this, on the other hand I did not ask him about this.” This is proof that the suspension was already known before Cardanus and was only called the “cardan suspension” after this description [1.2]. Translated from the Latin by Theodor Straub, Ingolstadt. Photograph: Deutsches Museum, Munich

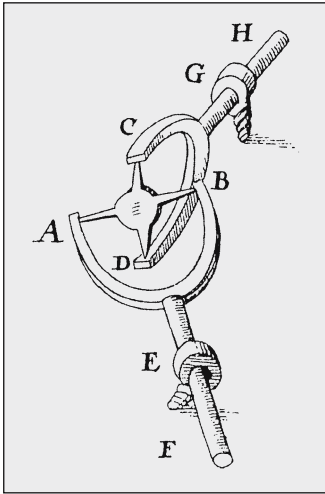


Fig. 1.2. Universal joint of Amicus (16th century). *ABCD* is a cross, the opposing arms *AB* of which are fitted into holes on the ends of a fork *ABF* (fusicula). The other pair of arms *CD* is received in the same way by the fork *CDH* and the forks themselves are mounted in fixed rings *G* and *E* [1.3, 1.7]. Photograph: Deutsches Museum, Munich

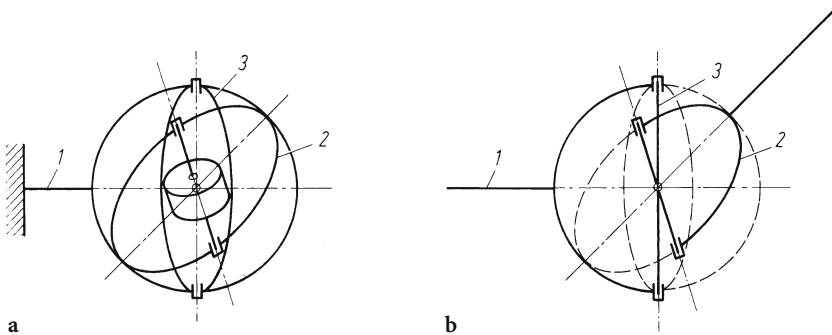


Fig. 1.3a, b. Relationship between gimbal and universal joint. **a** swiveling gimbal, the so-called “cardan suspension” (16th century). *1* attachment, *2* revolving ring, *3* pivot ring; **b** universal joint of Amicus (17th century), extended to make the cardan suspension. *1* drive fork, *2* driven fork, *3* cross

Johannes Hevelius, which comprised a universal joint similar to that of Amicus (Fig. 1.4). In 1676 he spoke of a “joynt” and a “universal joynt” because it is capable of many kinds of movements [1.5–1.7].

Hooke was fully conversant with the mathematics of the time and was also skilled in practical kinematics. In contrast to Schott he knew that the universal joint does not transmit the rotary movement evenly. Although Hooke did not publish any theory about this we must assume that he knew of the principle of the non-uniformity. He applied his joint for the first time to a machine with which he graduated the faces of sun dials (Fig. 1.5).

Cardano and Hooke can therefore be considered as having prepared the way for universal joints and driveshafts. The specialised terms “cardan joint” in Continental Europe and “Hooke’s joint” in Anglo-Saxon based languages still remind us of the two early scholars.

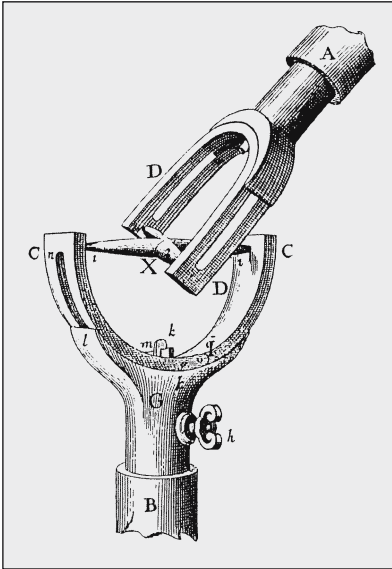


Fig. 1.4. Universal joint from the helioscope by Johannes Hevelius [1.5, 1.7]. Photograph: Deutsches Museum, Munich

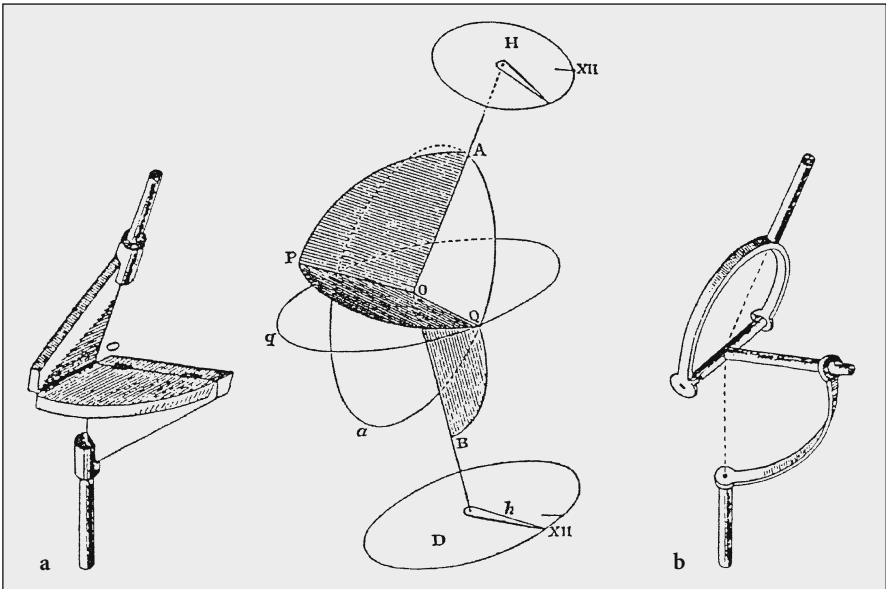


Fig. 1.5a, b. Principle of the apparatus for graduating the faces of sun dials, according to Robert Hooke 1674 [1.11]. a Double hinge of the dividing apparatus in a shaft system, as in b; b relationship between the universal joint and this element. Photograph: Deutsches Museum, Munich

1.2 Theory of the Transmission of Rotational Movements by Hooke's Joints

Gaspard Monge established the fundamental principles of his Descriptive Geometry in 1794 at the École Polytechnique for the study of machine parts in Paris. The most important advances then came in the 19th century from the mathematician and engineer officer Jean-Victor Poncelet, who had taught applied mathematics and engineering since 1824 in Metz at the Ecole d'Application, at a time when mechanical, civil and industrial engineering were coming decisively to the fore. As the creator of projective geometry in 1822 he perceived the spatial relationships of machine parts so well that he was also able to derive the movement of the Hooke's joint [1.8, 1.9]. It was used a great deal at that time in the windmills of Holland to drive Archimedes screws for pumping water.

1.2.1 The Non-Uniformity of Hooke's Joints According to Poncelet

In 1824 Poncelet proved, with the aid of spherical trigonometry, that the rotational movement of Hooke's joints is non-uniform (Fig. 1.6a and b).

Let the plane, given by the two shafts CL and CM , be the horizontal plane. The starting position of the cross axis AA' is perpendicular to it¹. The points of reference $ABA'B'$ of the cross and the yokes move along circles on the surface of the sphere K with the radius $AC = BC = A'C = B'C$. The circular surface $EBE'B'$ stands perpendicular to the shaft CL and the circular surface $DAD'A'$ to the shaft CM . The angle of inclination DCE of these surfaces to one another is the angle of articulation β of the two shafts CL and CM .

The relationships between the movements were derived by Poncelet from the spherical triangle ABE in Fig. 1.6b. If the axis CM has rotated about the arc $EA = \varphi_1$

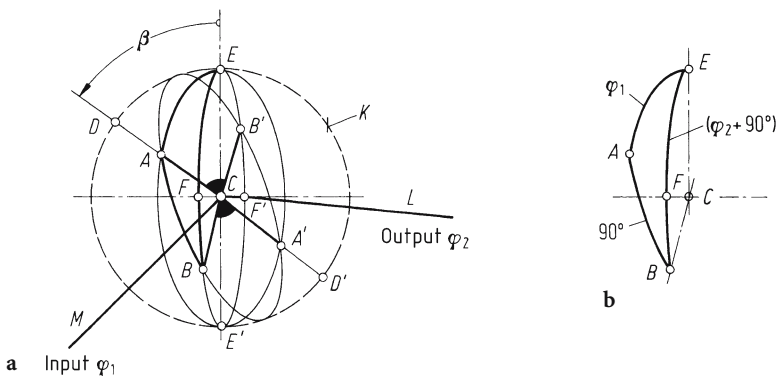


Fig. 1.6a, b. Proof of the non-uniform rotational movement of a Hooke's joint by J. V. Poncelet 1824. **a** Original figure [1.8, 1.9]; **b** spherical triangle from **a**

¹ Following the VDI 2722 directive of 1978 this is called "orthogonal". If AA' lies in the plane of the shaft then the starting position is "in-phase" [2.14].

while the axis CL turns about the arc $FB = \varphi_2$ then according to the cosine theorem [1.10, Sect. 3.3.12, p. 92]

$$\cos 90^\circ = \cos \varphi_1 \cos(90 + \varphi_2) + \sin \varphi_1 \sin(90 + \varphi_2) \cos \beta.$$

Since $\cos 90^\circ = 0$ it follows that

$$0 = \cos \varphi_1 (-\sin \varphi_2) + \sin \varphi_1 \cos \varphi_2 \cos \beta.$$

After dividing by $\cos \varphi_1 \sin \varphi_2$ Poncelet obtained

$$\tan \varphi_2 = \cos \beta \tan \varphi_1 \quad (1.1a)$$

or

$$\varphi_2 = \arctan(\cos \beta \tan \varphi_1). \quad (1.1b)$$

For the in-phase starting position, with $\varphi_1 + 90^\circ$ and $\varphi_2 + 90^\circ$ (1.1a). The following applies

$$\tan(\varphi_2 + 90^\circ) = \cos \beta \tan(\varphi_1 + 90^\circ) \Rightarrow \cot \varphi_2 = \cos \beta \cot \varphi_1$$

or

$$\frac{1}{\tan \varphi_2} = \cos \beta \frac{1}{\tan \varphi_1} \Rightarrow \tan \varphi_2 = \frac{\tan \varphi_1}{\cos \beta}. \quad (1.1c)$$

The *first derivative* of (1.1b) with respect to time gives the angular velocity

$$\begin{aligned} \frac{d\varphi_2}{dt} &= \frac{1}{1 + \tan^2 \varphi_1 \cos^2 \beta} \frac{\cos \beta}{\cos^2 \varphi_1} \frac{d\varphi_1}{dt} \\ &= \frac{\cos \beta}{\cos^2 \varphi_1 + \sin^2 \varphi_1 (1 - \sin^2 \beta)} \frac{d\varphi_1}{dt} \\ \frac{d\varphi_2}{dt} &= \frac{\cos \beta}{1 - \sin^2 \varphi_1 \sin^2 \beta} \frac{d\varphi_1}{dt} \quad [1.10, \text{Sect. 4.3.3.13, p. 107}] \end{aligned}$$

or because $d\varphi_2/dt = \omega_2$ and $d\varphi_1/dt = \omega_1$

$$\frac{\omega_2}{\omega_1} = \frac{\cos \beta}{1 - \sin^2 \beta \sin^2 \varphi_1}. \quad (1.2)$$

Equations (1.1a–c) and (1.2) form the basis for calculating the angular difference shown in Fig. 1.7a:

$$\Delta\varphi = \varphi_2 - \varphi_1$$

and the ratio of angular velocities ω_2/ω_1 shown in Fig. 1.7b.

For the two boundary conditions, (1.2) gives

$$\varphi_2 = 0^\circ, \quad \varphi_1 = 90^\circ \Rightarrow \omega_2 = \omega_{\min} = \omega_1 \cos \beta,$$

$$\varphi_2 = 90^\circ, \quad \varphi_1 = 180^\circ \Rightarrow \omega_2 = \omega_{\max} = \omega_1 / \cos \beta.$$

Figure 1.7a shows that an articulation of 45° gives rise to a lead and lag $\Delta\varphi$ about $\pm 10^\circ$, and very unpleasant vibrations ensue. The reduction of these vibrations has been very important generally for the mechanical engineering and the motor

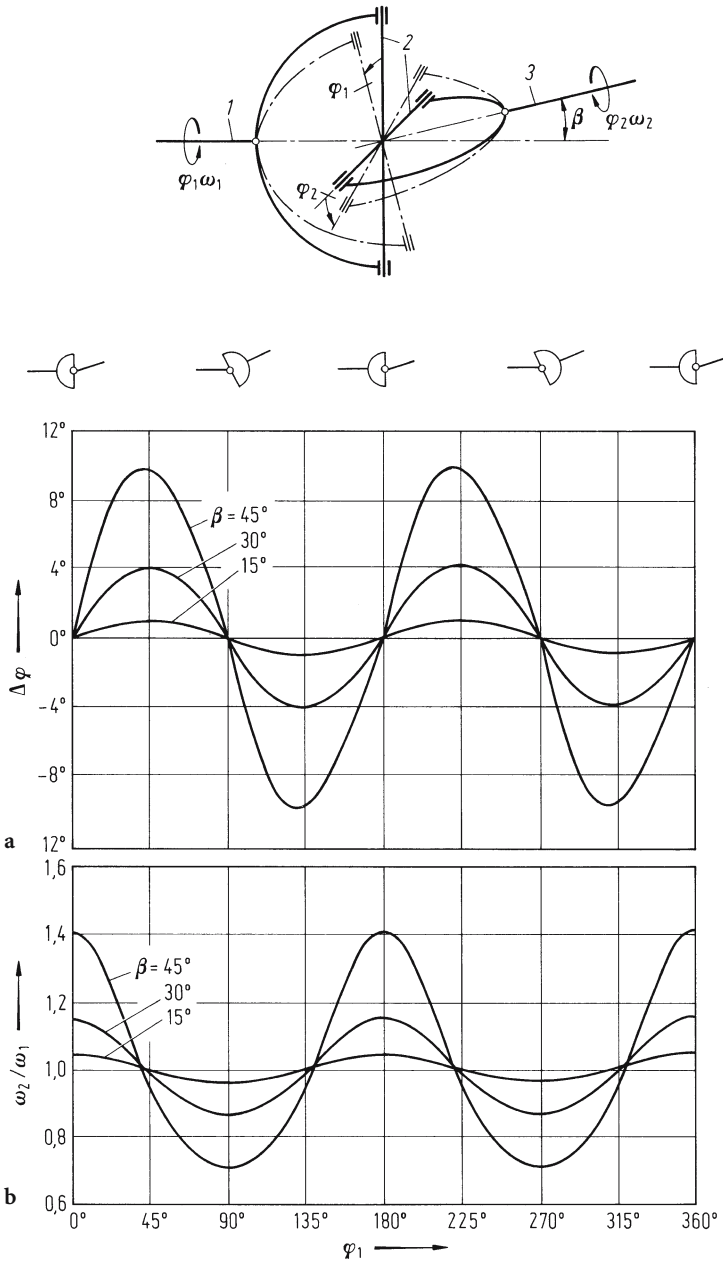


Fig. 1.7a, b. Angular difference and angular velocities of Hooke's joints for articulation angles of 15°, 30° and 45°. Single Hooke's joint (schematically) [1.36]. 1 Input shaft; 2 intermediate member (cross); 3 output shaft. ω_1 , ω_2 angular velocities of the input and output shafts, β angle of articulation, φ_1 , φ_2 angle of rotation of the input and output shafts. **a** Angular difference $\Delta\varphi$ (cardan error); **b** angular velocities. Graph of the angular velocity ω_2 for articulation angles of 15°, 30° and 45°

vehicle industries: for the development of front wheel drive cars it has been imperative. $\Delta\varphi$ is also called the angular error or “cardan error”.

The *second derivative* of (1.1b)

$$\frac{d\varphi_2}{dt} = \frac{d\varphi_1}{dt} \frac{\cos\beta}{1 - \sin^2\beta \sin^2\varphi_1} = \frac{k'}{1 - k^2 \sin^2\varphi_1}$$

with respect to time gives the angular acceleration

$$\begin{aligned} \alpha_2 &= \frac{d^2\varphi_2}{dt^2} = \frac{d\varphi_1}{dt} k' \frac{0(1 - k^2 \sin^2\varphi_1) - 1(-k^2 2\sin\varphi_1 \cos\varphi_1)}{(1 - k^2 \sin^2\varphi_1)^2} \frac{d\varphi_1}{dt} \\ &= \left(\frac{d\varphi_1}{dt}\right)^2 \frac{k' k^2 2\sin\varphi_1 \cos\varphi_1}{(1 - k^2 \sin^2\varphi_1)^2} = \omega_1^2 \frac{\cos\beta \sin^2\beta \sin 2\varphi_1}{(1 - \sin^2\beta \sin^2\varphi_1)^2}. \end{aligned} \quad (1.3)$$

This angular acceleration α_2 will be required in Sect. 4.2.7, for calculating the resulting torque, and for the maximum values of speed and articulation $n\beta$.

1.2.2 The Double Hooke’s Joint to Avoid Non-uniformity

In 1683 Robert Hooke had the idea of eliminating the non-uniformity in the rotational movement of the single universal joint by connecting a second joint (Fig. 1.8). In this arrangement of two Hooke’s joints the yokes of the intermediate shaft which rotates at ω_2 lie in-phase, i.e. as shown in Figs. 1.8, 1.9a and b in the same plane, as Robert Willis put forward in 1841 [1.11].

For joint 2 φ_2 is the driving angle and φ_3 is the driven angle. Therefore from (1.1c) $\tan\varphi_3 = \tan\varphi_2/\cos\beta_2$. Using (1.1c) one obtains

$$\tan\varphi_3 = \frac{\cos\beta_1 \tan\varphi_1}{\cos\beta_2}.$$

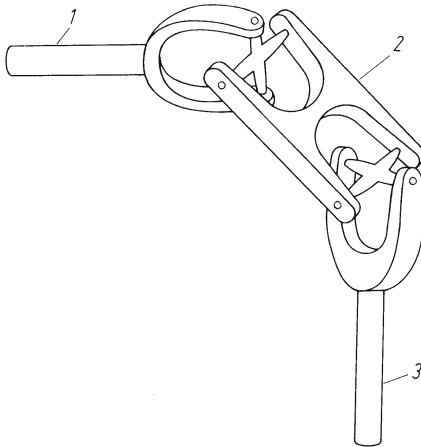


Fig. 1.8. Robert Hooke’s double universal joint of 1683 [1.6]. 1 Input, 2 intermediate part, 3 output

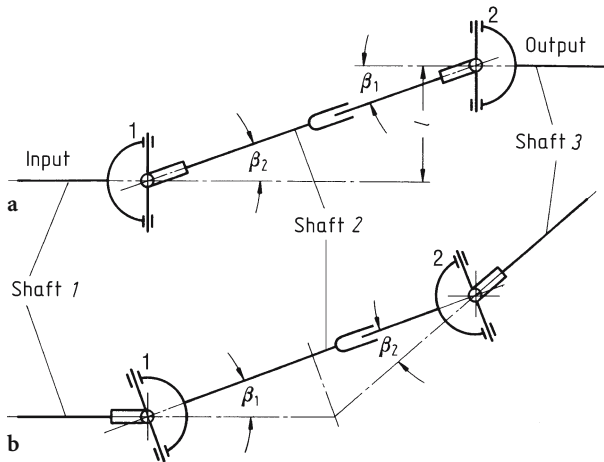


Fig. 1.9a, b. Universal joints with in-phase yokes and $\beta_1 = \beta_2$ as a precondition for constant velocity $\omega_3 = \omega_1$ [1.37]. a Z-configuration, b W-configuration

From this uniformity of the driving and driven angles then follows for the condition $\beta_2 + \pm \beta_1$, because $\cos(\pm \beta)$ gives the same positive value in both cases. Therefore $\tan \varphi_3 = \tan \varphi_1$ both in the Z-configuration in Fig. 1.9a and in the W-configuration in Fig. 1.9b, and also in the double Hooke's joint in Fig. 1.8. It follows that if $\varphi_3 = \varphi_1$

$$d\varphi_3/dt = d\varphi_1/dt \quad \text{or} \quad \omega_3 = \omega_1 = \text{const.} \quad (1.4)$$

Driveshafts in the Z-configuration are well suited for transmitting uniform angular velocities $\omega_3 = \omega_1$ to parallel axes if the intermediate shaft 2 consists of two prismatic parts which can slide relative to one another, e.g. splined shafts. The intermediate shaft 2 then allows the distance l to be altered so that the driven shaft 3 which revolves with $\omega_3 = \omega_1$ can move in any way required, which happens for example with the table movements of machine tools.

Arthur Hardt suggested in 1901 a double Hooke's joint in the W-configuration for the steering axle of cars (DRP 136605), "...in order to make possible a greater wheel lock...". He correctly believed that a single Hooke's joint is insufficient to accommodate on the one hand variations in the height of the drive relative to the wheel, and on the other hand sharp steering, up to 45° , with respect to the axle. For this reason he divided the steer angle over two Hooke's joints, the centre of which was on the axis of rotation of the steering knuckle, "... as symmetrical as possible to this ... in order to achieve a uniform transmission ...". Hardt saw here the possibility of turning the inner wheel twice as much as with a single Hooke's joint.

If, however, the yokes of the intermediate shaft 2 which revolves at ω_3 are out of phase by 90° then the non-uniformity in the case of shaft 3 increases to

$$\omega_{\max} = \frac{\omega_{\min}}{\cos \beta_1 \cos \beta_2},$$

which can be deduced in a similar way to (1.4).

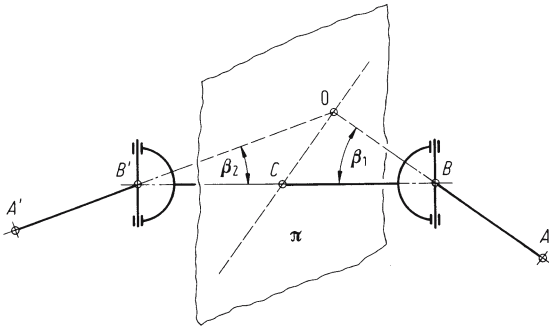


Fig. 1.10. Showing the constant velocity conditions for double Hooke's joints, according to d'Ocagne 1930 [1.14]

1.2.3 D'Ocagne's Extension of the Conditions for Constant Velocity

Is the condition $\beta_2 = \pm \beta_1$ sufficient for constant velocity? In 1841 Robert Willis deduced that the double Hooke's joint possesses constant velocity properties, even when the input and output shafts are neither parallel nor intersecting [1.11]. On these spatially oriented shafts constant velocity can only be achieved if the drive and driven axes are fixed. The yokes of the intermediate shaft 2 must be oppositely phased and disposed about the articulation angle φ according to the equation $\tan \varphi/2 = \tan \beta_2/\tan \beta_1$. In the case of planar axes $\beta_2 = \pm \beta_1$ can only be attained if the input and output shafts intersect one another. This was shown by Maurice d'Ocagne in 1918 [1.12]. According to his theory a double Hooke's joint only transmits in a uniform manner if, in accordance with Fig. 1.10, the following two conditions are fulfilled:

- the axes of the input and output shafts meet at the point O ,
- the two Hooke's joints are arranged symmetrically to a plane π which goes through points O and C .

These conditions are not so simple to fulfil in practice. Without special devices it is not possible to guarantee that the axes will always intersect and that the angle β_1 and β_2 are always the same. Figure 1.11a shows a modern design of double Hooke's joint without centring. There are however joint designs (Fig. 1.11b) in which the conditions are approximated (quasi-homokinetic joint) and some (Fig. 1.11c) where they are strictly fulfilled (homokinetic joint)². In 1971 Florea Duditza dealt with these three cases with the methods of kinematics [1.13].

1.2.4 Simplification of the Double Hooke's Joint

The quasi-homokinetic and also the strictly homokinetic double Hooke's joint as shown in Fig. 1.11b and c are complicated engineering systems made up of many dif-

² The term "homokinetic" (homo = same, kine = to move) was originated by two Frenchman Charles Nugue and Andre Planiol in the 1920s.

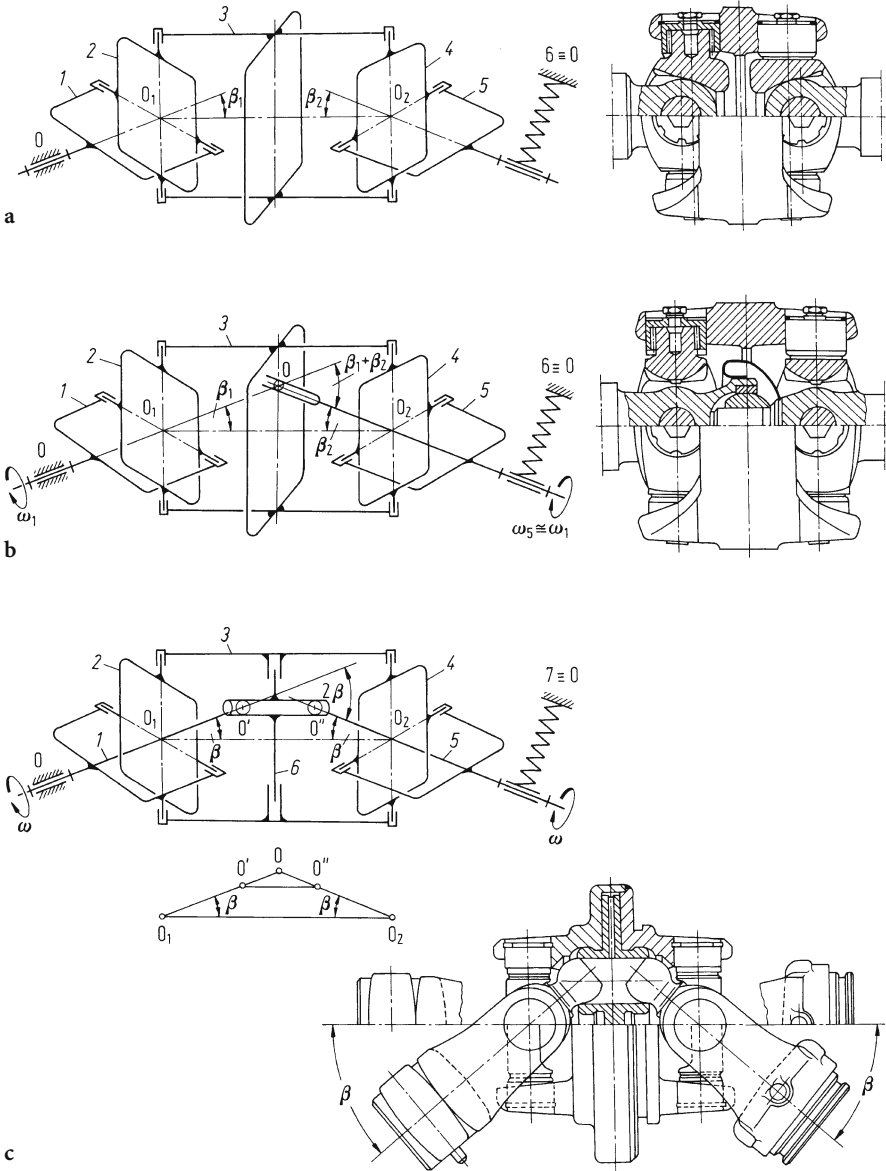


Fig. 1.11a–c. Various designs of double Hooke's joints. **a** Double Hooke's joint without centring. GWB design; **b** double Hooke's joint with centring (quasi-homokinetic), GWB design; **c** double Hooke's joint with steering attachment (strictly homokinetic) according to Paul Herchenbach (German patent 2802 572/1978), made by J. Walterscheid GmbH [2.14]

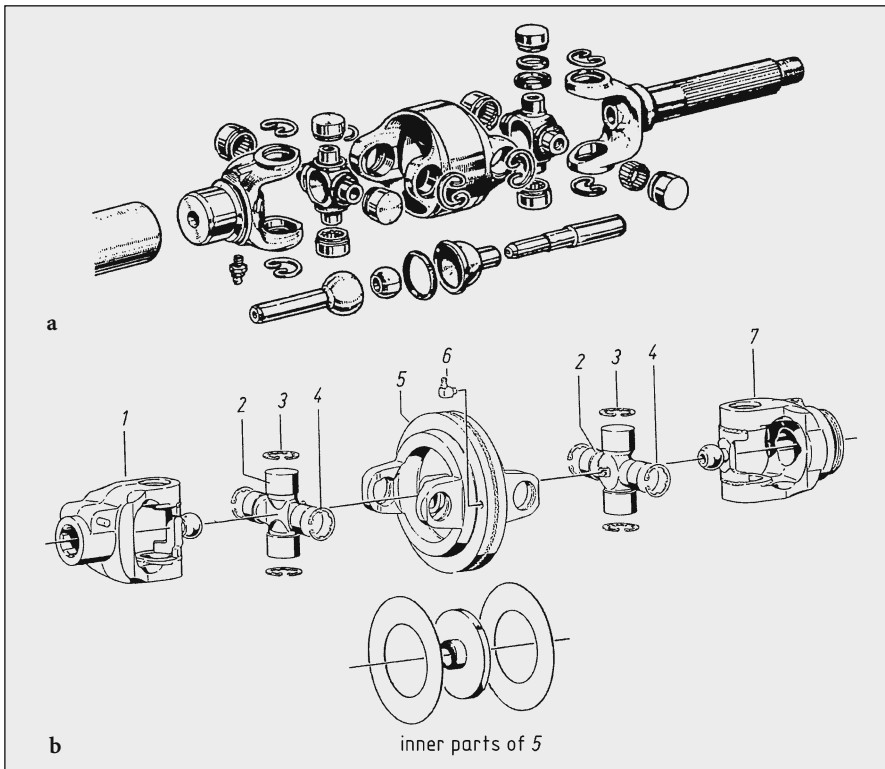


Fig. 1.12a, b. Exploded views of double Hooke's joints. **a** Citroën design with needle bearings and centring, 1934. Quasi-homokinetic, $\beta = 40^\circ$; **b** Walterscheid design by Hubert Geisthoff, Heinrich Welschof and Paul Herchenbach 1966–78 (German patent 1302735, 2802572). Fully-homokinetic, $\beta = 80^\circ$. 1 ball stud yoke; 2 unit pack; 3 circlip; 4 circlip for double yoke; 5 double yoke; 6 right angled grease nipple; 7 inboard yoke/guide hub

ferent elements (Fig. 1.12a and b). The task of finding simpler and cheaper solutions with constant velocity properties has occupied inventors since the second decade of this century. The tracta joint of Pierre Fenaille 1926 has had the best success [1.14, 1.15].

1.2.4.1 Fenaille's Tracta Joint

The Tracta joint works on the principle of the double tongue and groove joint (Fig. 1.13a–c). It comprises only four individual parts: the two forks F and F' and the two sliding pieces T and M (centring spheres) which interlock. These two sliding pieces, guided by spherical grooves, have their centre points C always the same symmetrical distance from the centre of the joint O . Constant velocity is thus ensured; independently of the angle of articulation the plane of symmetry π passes at $\beta/2$ through O . In 1930 Maurice d'Ocagne proved the constant velocity properties of the Tracta joint before the Academie des Sciences in Paris (Fig. 1.13b) [1.14].